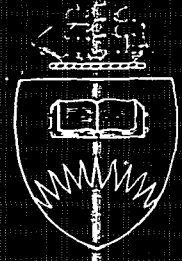

The Flinders University of South Australia

ELECTRONIC STRUCTURE OF MATERIALS CENTRE

Calculation of electron scattering on excited states of sodium

Igor Bray, Dmitry V. Fursa and Ian E. McCarthy

VOL 27 № 11

ESM-65

November 1993

submitted to Phys. Rev. A

Calculation of electron scattering on excited states of sodium

Igor Bray*, Dmitry V. Fursa and Ian E. McCarthy

Electronic Structure of Materials Centre, The Flinders University of South Australia, G.P.O. Box 2100, Adelaide 5001, Australia

(November 10, 1993)

Abstract

We present results of electron-sodium scattering for the $3D \rightarrow 3P$ transition at the projectile energy of 5 eV calculated using the Convergent Close-Coupling (CCC) method. These include spin-resolved and spin-averaged alignment, orientation, and coherence parameters, as well as differential cross section and spin asymmetry. This calculation simultaneously produces results for the transitions $3P \rightarrow 3P$ at 6.52 eV and $3S \rightarrow 3P$ at 8.62 eV, which are also presented. The three transitions are used to study the nature of the convergence in the close-coupling expansion. We find our results to be in excellent agreement with experiment, where available.

34.80.Bm, 34.80.Dp, 34.80.Nz

Typeset using REVTEX

I. INTRODUCTION

The Convergent Close-Coupling (CCC) method for electron scattering on hydrogen-like targets, those that may be readily treated by the model of a single valence electron above a frozen Hartree-Fock core, has been recently given by Bray [1]. This method treats these scattering systems as three-body problems, and expands the total wave function in a large truncated Laguerre basis enabling the application of standard close-coupling techniques to the resultant coupled equations. The method is applicable at all projectile energies and transitions of interest in atomic physics. Its utility relies on being able to achieve convergence to required accuracy with ever increasing basis sizes. This we are usually able to achieve using local computational facilities comprising desktop workstations. We consider the method to be complete in the sense that it provides simultaneously elastic, excitation, ionization, and therefore total cross sections for electron scattering from any particular target state.

For targets such as atomic hydrogen or the He^+ ion the CCC method is without approximation (suitability of the non-relativistic formalism is assumed) as the core consists of just the nucleus. Some of the most significant successes of the method are the excellent agreement with the measurements of the total ionization cross section by electron impact of atomic hydrogen [2] and of He^+ [3]. The method also works very well for positron scattering at energies where positronium formation is negligible [4,5]. Another most important success of the method is application to the Poet-Temkin model of electron-hydrogen scattering that treats only states with zero orbital angular momentum, which has been solved to a high accuracy [6,7]. It was shown [8] that the CCC method yielded correct convergent results, and that pseudoresonances, typically associated with square-integrable treatments of the continuum, diminish and disappear with increasing basis sizes. A disappointment for us is the inability of the method to have resolved the long-standing discrepancies between theory and experiment for the angular correlation parameters in electron-hydrogen [9].

The discrepancy with the angular correlation parameters for the atomic hydrogen target was one of primary reasons for generalization of the method to hydrogen-like targets. Ap-

plication to electron scattering on sodium [1], where there exist a great deal more detailed data, showed that the CCC method was able to obtain quantitative agreement with most experiments. In particular, excellent quantitative agreement was obtained with nearly all of the spin-resolved measurements available at the wide projectile energy range of 1 to 54 eV. The method is the only one that is able to achieve this to date, and improves significantly on the previous best Coupled-Channels Optical (CCO) theory of Bray and McCarthy [10]. Such excellent agreement with experiment for the sodium target, particularly with those parameters where there is considerable discrepancy in the atomic hydrogen target, gives us considerable confidence in the CCC method.

The earlier work [1] concentrated only on those transitions involving the ground state. This is because its purpose was to demonstrate validity of the method by comparison with the large volume of experimental data which exists for these transitions. For the same reason we found it impractical to provide a detailed analysis of the nature of convergence. The aim of this paper is to demonstrate that the CCC method also works for transitions involving only excited states, and to provide a considerable amount of information about convergence, as a function of increasing basis sizes, for various observables and transitions of interest. We concentrate on just a single projectile energy of 5 eV relative to the $3D$ state of sodium. It is for the $3D \rightarrow 3P$ transition at this energy that there exists considerable data, presented in the review of Anderson, Gallagher, and Hertel [11]. This energy is a few eV above the ionization threshold, and so lies in the most difficult intermediate energy range, providing an excellent opportunity for study of convergence. By the very nature of the close-coupling (CC) formalism, we are able to simultaneously calculate those transitions that have the same total energy (relative to the inert core). The ones we choose to present here are the $3P \rightarrow 3P$ at 6.52 eV and $3S \rightarrow 3P$ at 8.62 eV. All three of these transitions have the same total energy of 3.48 eV.

II. THEORY

The scattering formalism for electron scattering on hydrogen-like targets has been given earlier [1]. This work concentrated only on those transitions which involved the ground state. In this work we interested in scattering between excited states, and in particular, to the $3P$ state from any other state. We therefore need to present the relations between the scattering amplitudes that may be obtained from the CCC calculations, and the alignment, orientation, and coherence parameters for the transitions of interest.

In the laboratory this information may be obtained in the time-reversed process. In experiments of this type, the sodium atom is first laser excited from the ground $3^2S_{1/2}, F = 2$ state into a particular combination of the hyperfine state magnetic sublevels M_F of the $3^2P_{3/2}, F = 3$ state. The differential cross sections to any other state, on electron excitation, are then measured for varying polarizations of the laser light. We suppose that the hyperfine interaction plays no essential role during electron scattering and neither does spin-orbit interaction (the Percival-Seaton hypothesis) [12]. It has been shown [11,13] that cross section measurements for electron scattering on laser excited atoms are equivalent to the time reversed coincidence experiments. We present spin-resolved and spin-averaged orientation and alignment parameters as well as differential cross sections and spin asymmetries for the excitation of the sodium $3P$ state from the $3S$, $3P$, and $3D$ states. We use these to examine convergence in the CCC method.

The CCC calculations yield reduced T-matrix elements, which depend on the total spin S and partial waves of total orbital angular momentum J, for various transitions of interest. The total spin S is assumed to be conserved in the $L - S$ coupling scheme and is zero for singlet and unity for triplet scattering. Convergence, as a function of basis size, may be studied by directly comparing corresponding T-matrix elements, as we have done for electron scattering on atomic hydrogen [9]. However, on occasion a small variation in the T-matrix elements may lead to a larger variation in an observable [9], and so we concentrate here on discussing convergence by looking at the resulting experimentally derivable quantities.

The reduced T-matrix elements may be related to the scattering amplitudes in the collision frame, where the the quantization axis is along the incident projectile, by

$$f^S_{m_f m_i}(\theta,\varphi) = \frac{1}{4\pi}\frac{1}{\sqrt{2l_i+1}}\sqrt{\frac{k_i}{k_f}}\sum_{L_f,L_i,J}(2L_i+1)C^{m_i-m_f\,m_f\,m_i}_{L_f\quad l_f\quad J} \times C^{0\;m_i m_i}_{L_i l_i\;J} T^{JS}_{l_i l_f L_i L_f} Y^{L_f *}_{m_i-m_f}(\theta,\varphi), \tag{1}$$

where l_i, m_i and l_f, m_f are the orbital angular momentum and its projection of the initial and final states, respectively. The initial and final linear and orbital angular momenta of the projectile are denoted by k_i, L_i and k_f, L_f. As we are only interested in electron measurements performed in the scattering plane, we set $\varphi = 0$ and drop it from the notation.

All experimentally observable quantities may be related to the scattering amplitudes. The spin-resolved differential cross section is given by

$$\sigma^S(\theta) = \sum_{m,m'} |f^S_{mm'}(\theta)|^2, \tag{2}$$

and the spin-averaged differential cross section is given by

$$\sigma(\theta) = \sum_S \frac{2S+1}{4}\sigma^S(\theta). \tag{3}$$

Assuming that the initial target state is unpolarised, the spin-dependent density matrix of the final $3P$ state, normalized to unity trace, is [14]

$$\rho^S_{mm'}(\theta) = \sum_{m_i} f^S_{mm_i}(\theta) f^{S*}_{m'm_i}(\theta)/\sigma^S(\theta), \tag{4}$$

which may be used to obtain the spin-averaged density matrix

$$\rho_{mm'}(\theta) = (\rho^0_{mm'}(\theta) + 3r(\theta)\rho^1_{mm'}(\theta))/(1+3r(\theta)), \tag{5}$$

where

$$r(\theta) = \sigma^1(\theta)/\sigma^0(\theta) \tag{6}$$

is the ratio of triplet to single differential cross sections. This ratio is often expressed as an exchange asymmetry via

$$A_{ex} = \frac{1-r}{1+3r}, \tag{7}$$

which has the advantage of always being finite. The spin-averaged state multipoles T_{kq} are related to the density matrix by [14]

$$T_{kq}(\theta) = \sum_{m,m'} (-1)^{l_f - m} C^{m'-mq}_{l_f\ l_f\ k} \rho_{mm'}(\theta). \tag{8}$$

The spin-dependent state multipoles T^S_{kq} are obtained by using the spin-dependent density matrix in the above relation.

Reduced Stokes parameters P_1, P_2, P_3 are used to describe the atomic charge cloud after electron excitation [11], and depend only on the collison dynamics. These are related to the state multipoles via

$$P_1 = \frac{\alpha_2(T_{22} - \sqrt{\frac{3}{2}}T_{20})/2}{T_{00} - \frac{\alpha_2}{2}(\frac{T_{20}}{\sqrt{6}} + T_{22})}, \tag{9}$$

$$P_2 = \frac{\alpha_2 T_{21}}{T_{00} - \frac{\alpha_2}{2}(\frac{T_{20}}{\sqrt{6}} + T_{22})}, \tag{10}$$

$$P_3 = -\frac{\alpha_1 i T_{11}}{T_{00} - \frac{\alpha_2}{2}(\frac{T_{20}}{\sqrt{6}} + T_{22})}, \tag{11}$$

where the coefficients α_k are

$$\alpha_k = 3(2l_1+1)^{1/2}(-1)^{l_i+l_2+k+1} \begin{Bmatrix} 1 & l_1 & l_2 \\ l_1 & 1 & k \end{Bmatrix}, \tag{12}$$

and where the braces indicate the Wigner $6-j$ symbol. For scattering to the $3P$ state, $l_1 = l_f = 1$ and $l_2 = 0$ due to the dipole photon deexcitation. In this case $\alpha_k = \sqrt{3}, k = 1, 2$. When scattering with $l_i = 0$ further simplification is possible. The symmetry property of the scattering amplitudes $f^S_{10} = -f^S_{-10}$ results in the additional relation for the state multipoles [13]

$$T_{20}/\sqrt{6} + T_{22} = -1/3 \tag{13}$$

and the reduced Stokes parameters are then given by

$$P_1 = 1 + 4T_{22}, \tag{14}$$

$$P_2 = 2T_{21}, \tag{15}$$

$$P_3 = -2iT_{11}. \tag{16}$$

A more physical description of the charge cloud is provided by the alignment, orientation, and coherence parameters [11]. The linear polarization of the atomic charge cloud is

$$P_\ell = (P_1^2 + P_2^2)^{1/2}, \tag{17}$$

the alignment angle relative to the z axis of the collision frame is

$$\gamma = \arg(P_1 + iP_2)/2, \tag{18}$$

the angular momentum transferred to the atom perpendicular to the scattering plane is

$$L_\perp = 2iT_{11} \tag{19}$$

and the degree of polarization (total coherence) is

$$P^+ = (P_1^2 + P_2^2 + P_3^2)^{1/2}. \tag{20}$$

In the case of $S \rightarrow P$ scattering the measurement of only the three Stokes parameters allows us to determine state multipoles T_{kq} unambiguously. In this case $L_\perp = -P_3$, and moreover there is complete coherence ($P^+ = 1$) in both singlet and triplet channels. However, in the general case it is necessary to define one more parameter. It is convenient to use the natural frame density matrix element [11]

$$\rho_{00}^n = \frac{1}{3} + T_{22} + \frac{T_{20}}{\sqrt{6}}. \tag{21}$$

It vanishes for $S \rightarrow P$ transitions due to symmetry properties (13), but is not zero in the general case. The orientation parameter $L_\perp$ can then be described in terms of experimentally derivable quantities only via

$$L_\perp = 2iT_{11} = -P_3(1 - \rho_{00}^n). \tag{22}$$

Spin resolved counterparts to the above defined parameters may be simply obtained by restoring the total spin S index to the state multipoles T_{kq}.

III. RESULTS

Our motivation for the application of the CCC method to scattering from excited states of sodium is primarily the existence of the $3D \rightarrow 3P$ data for alignment and orientation parameters at projectile energy of 5 eV presented by Anderson, Gallagher, and Hertel [11]. The nature of the method is such that in calculating this transition we simultaneously obtain results for other transitions having the same total energy of 3.48 eV. We present two of these, namely $3S \rightarrow 3P$ at 8.62 eV and $3P \rightarrow 3P$ at 6.52 eV. We use these three transitions to give a detailed discussion of establishment of convergence in the CCC method.

Ideally, we would be able to calculate the spin and magnetic sublevel dependent scattering amplitudes for any transition and projectile energy to an arbitrary accuracy. Unfortunately this is not the case. Though the CCC formalism suggests that this is possible in principle, in practice our computational resources put a limit on the size of the calculations.

For any transition and projectile energy of interest we need to establish convergence as a function of the size of the Laguerre basis for each target state orbital angular momentum l, and with increasing $l_{\max}$, the maximum value of l treated in the calculation. The size of the calculation depends on the set of linear equations formed when solving the coupled equations. The number of coupled equations is equal to the product of the number of channels N_c and the number of projectile momentum quadrature points N_k within each channel. Given a Laguerre basis size N_l the number of channels it generates is $(l+1)N_l$ for the "natural" parity, and lN_l for the "unnatural" parity [1]. Thus, assuming the same N_l for each l the maximum number of channels is given by $N_l(l_{\max}+1)(l_{\max}+2)/2$. This places a limitation on the transitions that may be studied.

In the intermediate energy range, where convergence with increasing N_l is likely to be slow, we are unable to provide accurate information that involves transitions with states having $l \geq 3$. These would require solutions of linear equations of order 10000×10000 which require at least 400M of core memory storage. For example, such large matrices would arise if we were to take $N_l = 13$ for each l, with around $N_k = 50$ in each channel, and

have $l_{max} = 4$. Here we assume that in order to be confident of a result involving transitions with say $l = 3$ for one of the states, we would require to be able to perform the calculation with at least $l_{max} = 4$. Demonstration of the requirement of having l_{max} at least one more than the l in the transitions considered is one of the issues we wish to address in this work.

Fortunately, most scattering transitions of interest in atomic physics do not involve very large l. Perhaps the most studied is the dipole s to p transition, for which we have little difficulty in obtaining quite accurate results at all projectile energies [1,9].

One way we may try to reduce the number of channels in the calculation is by not using the full set of N_l states that arise from the diagonalization of the target Hamiltonian. For example, for energies above the ionization threshold we may try to obtain convergence in the use of just those states that lead to open channels. To obtain convergence in the use of a subset of states is a stronger condition than convergence in the use of the full set of states. We restrict this procedure to projectile energies above the ionization threshold only because in this case we can be confident that an increase in the basis size will test the convergence in the use of both negative and positive energy target states. This works very well for the sodium target [1], but may not be the case for other targets, in particular whenever the continuum provides a considerable fraction of the target polarization.

To examine convergence in the CCC method we present four calculations in Figs. 1 to 9. The largest of these contains $12s$, $13p$, $13d$, and $11f$ states. The 49 states generate 121 channels for "natural" parity and 72 channels for the "unnatural" parity. In each channel we used 60 quadrature points. As the projectile energy is only a few eV (3.48) above the ionization threshold we used very large basis sizes for each target state l, but used only those states which generate open channels. In particular, we took $N_s = 40$, $N_p = 40$, $N_d = 40$, and $N_f = 30$. The exponential fall-off factors [1] were $\lambda_s = 2.4$, $\lambda_p = 2.0$, $\lambda_d = 2.0$, and $\lambda_f = 1.5$. For simplicity of discussion we shall refer to this as calculation a. The second largest calculation that we performed used $10s$, $12p$, $11d$, and $9f$ states. These were generated by reducing the above basis sizes for each l by five, whilst keeping the exponential fall-off factors the same. Only states leading to open channels were retained. We denote this

calculation by b. Comparison of calculations a and b indicates convergence as a function of basis sizes whilst keeping $l_{max} = 3$. The third calculation uses the same parameters as for a except that it has $l_{max} = 2$, and we denote it by c. Comparison of c with a indicates the effect of the inclusion of f states. The last calculation is a standard close-coupling calculation that is convergent in the use of just discrete target eigenstates. These are the first 15 discrete states comprising of $4s$, $4p$, $4d$, and $3f$ states. The effect of adding the lowest-lying two g states was found to be negligible. We denote this calculation by d, comparison with a and b shows the effect of the continuum.

In Fig. 1 we present the above-mentioned four calculations for the singlet parameters $L_\perp$, P_t, γ, ρ^n_{00}, P^+, as well as the exchange asymmetry A_{ex}, for the $3S \rightarrow 3P$ transition in electron-sodium scattering at 8.62 eV. For definition of these parameters see the previous section. Here we are able to compare with experiment for the $L_\perp$ and A_{ex} parameters, though the measurements of Scholten *et al.* [15] correspond to the energy of 10 eV, and find very good agreement. See Bray [1] for presentation of CCC calculations at 10 eV. The results for the singlet $L_\perp$ clearly indicate the importance of the continuum, as it is only calculation d, the one that contains just bound states, which doesn't give good agreement with experiment. We generally see quite small variation between the three calculations a, b, and c indicating good convergence in both basis sizes N_l and l_{max}. The exceptions to this are the P_t and γ near 120 degrees. The difference between calculations a and b here indicates a lack of convergence with N_l. If it was our interest to primarily present convergence in these parameters we would follow these calculations by reducing the number of f states and increasing the number of s, p and d states until convergence is achieved. The reason for the large number of f states used is that these prove to be necessary for the $3D \rightarrow 3P$ transition.

The triplet results for the above parameters are presented in Fig. 2, with the ratio of triplet to singlet scattering r being presented rather than the equivalent A_{ex} of the previous figure. All four calculations give very similar results and are in good agreement with available experiment, though we do see that very backward angles are particularly sensitive to

variation in the basis sizes. By comparing A_{ex} and r results near 120 degrees, it is interesting to see how different presentation of the same information can be. The large variation in r at these angles is due to the fact that the singlet differential cross section is at a minimum here which is nearly zero.

Corresponding spin-averaged results are given in Fig. 3. Here we see very good agreement between all of the theories indicating that convergence for spin-averaged parameters is often easier to obtain than for spin-resolved ones. We note that the total coherence parameter P^+ is no longer identically unity, but shows significant loss of coherence due to the effects of exchange.

In Figs. 4, 5, and 6 we look at the singlet, triplet, and spin-averaged elastic $3P \rightarrow 3P$ transition at projectile energy of 6.52 eV, respectively. Here we have contribution from T-matrix elements with the "unnatural" parity. We see that calculation d is often quite different from the others for all three spin states indicating the significance of the continuum. Variation between calculations a and c indicates that f states play a more important role here than above. Convergence at the backward angles is at times very difficult to achieve. The singlet and triplet parameters P^+ show loss of coherence due to the averaging over the initial magnetic sublevels. The spin-averaged P^+ has, in addition, loss of coherence due to exchange. The ρ^n_{00}, for singlet, triplet, and spin-averaged cases, are no longer zero due to the existence of transitions between states with negative reflection symmetry [11]. It is interesting to find that γ starts at $-\pi/2$ rather than at zero as in the $3S \rightarrow 3P$ transition.

In Figs. 7, 8, and 9 we look at the singlet, triplet, and spin-averaged $3D \rightarrow 3P$ transitions at projectile energy of 5 eV, respectively. It is for the averaged spin state that there are measurements for the parameters presented. Unfortunately, these only extend to 30 degrees, and so do not provide as strong as possible a test of theory. Nevertheless, we do find very good agreement with the measurements, and our theory is of considerable improvement on the Born approximation presented by Anderson, Gallagher, and Hertel [11], which yields identically zero for $L_\perp$, and gives wrong γ. Turning our attention to the discussion of convergence, we see that the difference between calculations a and c is often substantial

indicating the importance of the inclusion of f states. This confirms the desirability of having l_{max} at least one greater then the largest l in the transition of interest. Comparison of a and d shows significant effects of the continuum. Even the differential cross section is significantly affected by the inclusion of the continuum. The fact that the magnitude of $L_\perp$ is considerably smaller ($\ll 1$) than in the $3S \rightarrow 3P$ transitions results in the fact that P_ℓ and P^+ are very similar, as is the case for the $3P \rightarrow 3P$ transitions. The origin of γ has reverted to zero, but changes very rapidly with increasing scattering angle.

IV. CONCLUSION

We have presented results from four separate calculations in order to demonstrate the nature of convergence in the CCC method and its applicability to transitions involving only excited states at the most difficult projectile energy range of a few eV above the ionization threshold. Each calculation produces the results, presented in Figs. 1 to 9, simultaneously. Good agreement with experiment, where available, allows us to be confident in the presented results for those parameters and transitions where experiment is not available. For this reason we urge future experimental work to be performed at those projectile energies that lead to total energies at which there are already other reliable experimental data.

We found that convergence, to a particular accuracy, varies with transition, description parameter, and scattering angle. Spin-resolved parameters are usually more sensitive to basis sizes than are the corresponding spin-averaged ones. The $3D \rightarrow 3P$ transition is the most difficult due to the need for the inclusion of a large number of f states in the target expansion. We are unable to provide more accurate results than those presented for this transition due to the computational resources available to us. However, the other two transitions may be obtained more accurately by reducing the number of f states in the calculation and increasing the number of s, p and d states instead.

We would like to emphasize that any difficulty encountered in obtaining convergence in the CCC method is an indication of the difficulty of the problem, and not a failing of

the method. We are unaware of any other scattering theory which is able to provide more accurate information at any projectile energy or transition of interest.

Extension of the CCC method to electron-helium scattering and (e,2e) differential cross sections is under current investigation. We also plan to present data for scattering from targets where the initial state is polarized.

ACKNOWLEDGMENTS

We would like to acknowledge support from the Australian Research Council and The Flinders University of South Australia.

REFERENCES

* electronic address: igor@esm.ph.flinders.edu.au.

[1] I. Bray, (in press) Phys. Rev. A (1993).

[2] I. Bray and A. T. Stelbovics, Phys. Rev. Lett. **70**, 746 (1993).

[3] I. Bray, I. E. McCarthy, J. Wigley, and A. T. Stelbovics, submitted to J. Phys. B (1994).

[4] I. Bray and A. T. Stelbovics, (in press) Phys: Rev. A **48**, (1993).

[5] I. Bray and A. T. Stelbovics, (in press) Phys. Rev. A (1993).

[6] R. Poet, J. Phys. B **11**, 3081 (1978).

[7] A. Temkin, Phys. Rev. **126**, 130 (1962).

[8] I. Bray and A. T. Stelbovics, Phys. Rev. Lett. **69**, 53 (1992).

[9] I. Bray and A. T. Stelbovics, Phys. Rev. A **46**, 6995 (1992).

[10] I. Bray and I. E. McCarthy, Phys. Rev. A **47**, 317 (1993).

[11] N. Andersen, J. W. Gallagher, and I. V. Hertel, Phys. Rep. **165**, 1 (1988).

[12] I. C. Percival and M. J. Seaton, Proc. Cambridge Philos. Soc. **53**, 654 (1957).

[13] I. V. Hertel and W. Stoll, Adv. Atom. Mol. Phys. **13**, 113 (1977).

[14] K. Blum, *Density Matrix Theory and Applications* (Plenum Press, New York, 1981).

[15] R. E. Scholten *et al.*, J. Phys. B **24**, L653 (1991).

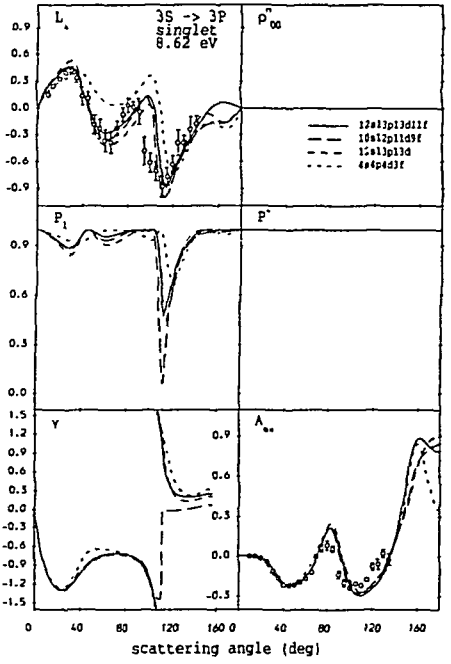

Fig. 1
Bray et al.
Phys. Rev. A

FIG. 1. Singlet alignment parameter $L_\perp$, orientation parameters P_ℓ and γ, coherence parameter P^+, the density matrix element in the natural frame ρ^n_{00}, and exchange asymmetry A_{ex} for electron scattering on the ground state of sodium at 8.62 eV. The presented measurements of Scholten *et al.* [15] correspond to the projectile energy of 10 eV. See text for detailed description of the theory. Quantitative results may be obtained by correspondence with the first author*.

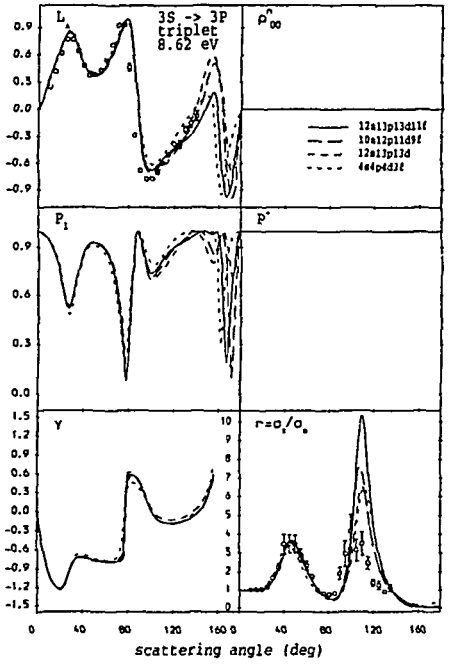

Fig. 2
Bray et al.
Phys. Rev. A

FIG. 2. Triplet alignment parameter $L_\perp$, orientation parameters P_ℓ and γ, coherence parameter P^+, the density matrix element in the natural frame ρ^n_{00}, and ratio r of triplet to sihglet scattering for electron scattering on the ground state of sodium at 8.62 eV. The presented measurements of Scholten *et al.* [15] correspond to the projectile energy of 10 eV. See text for detailed description of the theory.

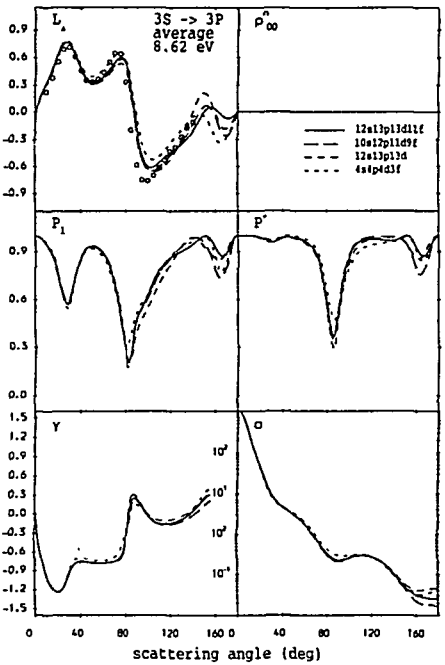

Fig. 3
Bray et al.
Phys. Rev. A

FIG. 3. Spin-averaged alignment parameter $L_\perp$, orientation parameters P_ℓ and γ, coherence parameter P^+, the density matrix element in the natural frame ρ^n_{00}, and differential cross section for electron scattering on the ground state of sodium at 8.62 eV. The presented measurements of Scholten *et al.* [15] correspond to the projectile energy of 10 eV. See text for detailed description of the theory.

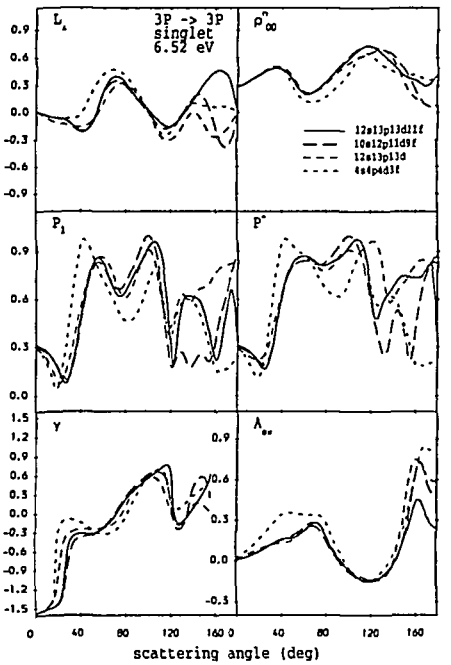

Fig. 4

Bray et al.

Phys. Rev. A

FIG. 4. As for figure 1, except for the indicated transition and projectile energy.

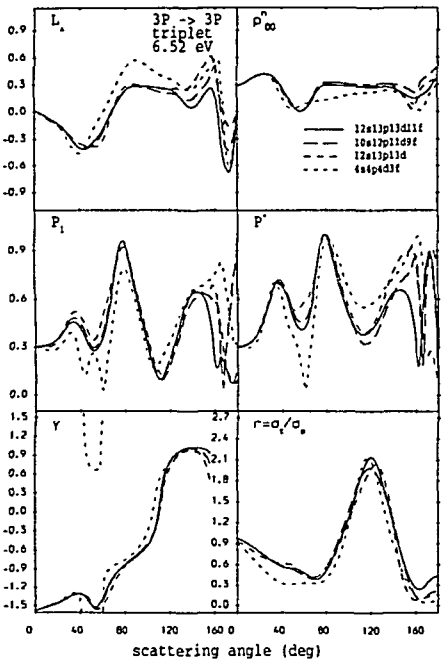

Fig. 5

Bray et al.

Phys. Rev. A

FIG. 5. As for figure 2, except for the indicated transition and projectile energy.

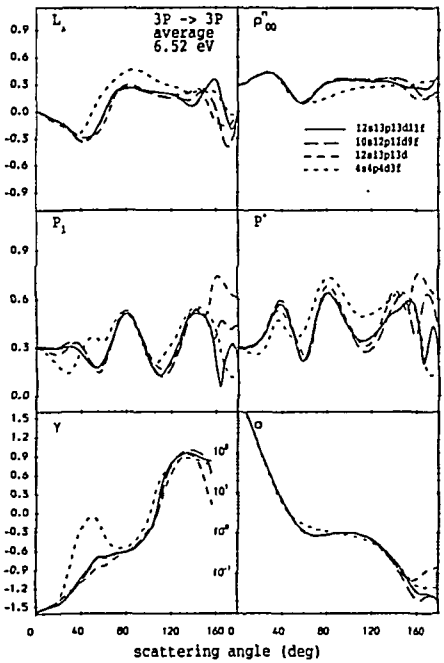

Fig. 6

Bray et al.

Phys. Rev. A

FIG. 6. As for figure 3, except for the indicated transition and projectile energy.

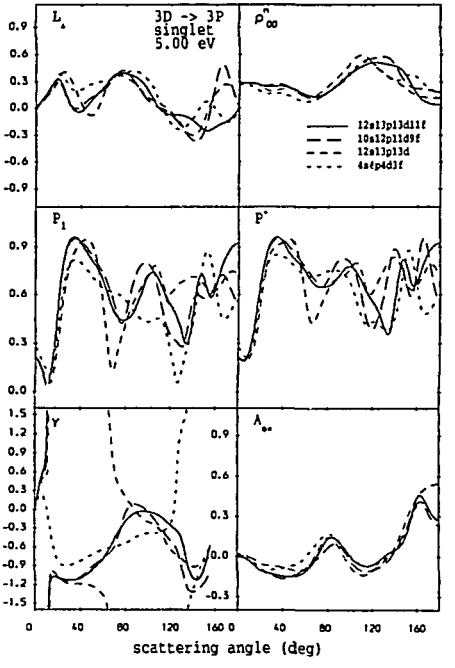

Fig. 7
Bray et al.
Phys. Rev. A

FIG. 7. As for figure 1, except for the indicated transition and projectile energy.

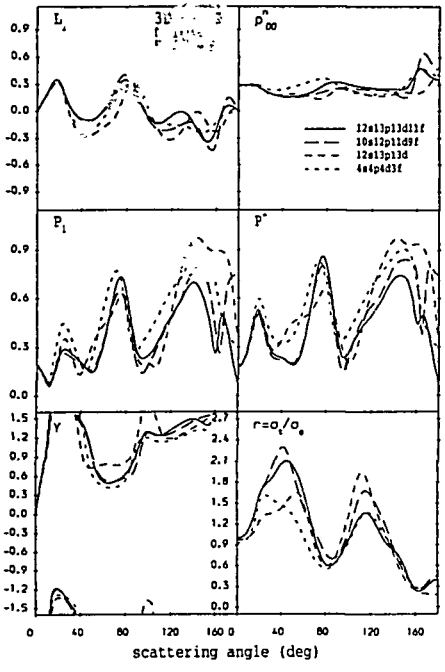

Fig. 8

Bray et al.

Phys. Rev. A

FIG. 8. As for figure 2, except for the indicated transition and projectile energy.

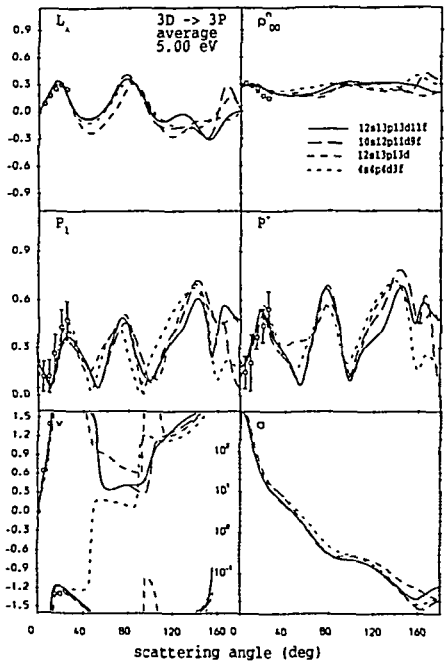

Fig. 9
Bray et al.
Phys. Rev. A

FIG. 9. As for figure 3, except for the indicated transition and projectile energy. The experimental data are from Anderson, Gallagher, and Hertel [11].